miR-383 increases the cisplatin sensitivity of lung adenocarcinoma cells through inhibition of the RBM24-mediated NF-κB signaling pathway

BO HE[1*], CHAO WU[1*], WEICHAO SUN[2], YANG QIU[1], JINGYAO LI[1],
ZHIHUI LIU[3], TAO JING[3], HAIDONG WANG[1] and YI LIAO[1]

[1]Department of Thoracic Surgery, Southwest Hospital, Army Medical University, Chongqing 400038; [2]The Central Laboratory,
Shenzhen Second People's Hospital, Shenzhen University First Affiliated Hospital, Shenzhen, Guangdong 518035;
[3]Department of Cardiology, Southwest Hospital, Army Medical University, Chongqing 400038, P.R. China

Abstract. The expression of microRNA-383 (miR-383) is downregulated in a variety of tumor tissues, and it exhibits antiproliferative activity in non-small cell lung cancer cells. In the present study, an association between the downregulation of miR-383 expression and the deletion of chr8p22 in patients with lung adenocarcinoma was identified. The promoting effect of miR-383 on cisplatin sensitivity was verified both *in vivo* and *in vitro*. Additionally, it was revealed that the expression of RNA binding motif protein 24 (RBM24) protein was regulated by and negatively correlated with miR-383 expression. Ectopic expression of RBM24 or inhibition of miR-383 decreased the chemosensitivity of parental A549 cells, whereas knockdown of RBM24 in cisplatin-resistant A549 cells increased chemosensitivity. Mechanistically, miR-383 interfered with the activation of nuclear factor κB (NF-κB) signaling through repression of RBM24-mediated phosphorylation of Rel-like domain-containing protein A and inhibitor α of NF-κB. Taken together, the downregulation of miR-383 induced RBM24 expression, which was mediated through the activation of NF-κB signaling, to contribute to chemotherapy resistance in lung adenocarcinoma cells. The results of the present study highlight potential therapeutic targets for the clinical reversal of the chemotherapy resistance in lung adenocarcinoma.

Correspondence to: Professor Haidong Wang or Dr Yi Liao, Department of Thoracic Surgery, Southwest Hospital, Army Medical University, 30 Gaotanyan Street, Chongqing 400038, P.R. China
E-mail: haidongwang1970@163.com
E-mail: science0528@163.com

*Contributed equally

Introduction

Non-small cell lung cancer (NSCLC) is the world's leading malignant tumor in terms of morbidity and mortality, of which, lung adenocarcinoma is the most common subtype (1,2). Surgical resection, chemotherapy and radiotherapy remain the primary treatment options for lung adenocarcinoma. In recent decades, despite improvements in diagnostics, surgical techniques and radiochemotherapy regimens, as well as the application of molecular targeted therapy, the long-term prognosis of patients with lung adenocarcinoma remains poor due to the high metastasis and recurrence rate, with a 5-year overall survival rate of <25% (3). Platinum based chemotherapy is the conventional treatment for lung adenocarcinoma (4). However, the effectiveness of chemotherapy is limited due to the development of chemoresistance (5), and the underlying molecular mechanisms of chemotherapeutic drugs used for lung adenocarcinoma are largely unknown, thus preventing resistance remains a considerable challenge.

MicroRNAs (miRNAs/miRs) are a large class of endogenous, small noncoding regulatory RNAs (~22 nucleotides in length) that can suppress the expression of multiple target genes by cleaving target mRNAs and/or inhibiting protein translation (6,7). Studies have demonstrated that miRNAs play critical roles in the initiation, progression and metastasis of various types of cancer (8-12). In addition, an increasing number of studies have suggested that miRNAs are significantly associated with chemosensitivity in cancer (13). For NSCLC cells, it has been reported that miR-185-5p can overcome cisplatin sensitivity by targeting ATP binding cassette subfamily C member 1 (14), and miR-106b-5p can reverse cisplatin resistance by suppressing the expression of polycystin 2 (15). Moreover, overexpression of miR-216b significantly increased the sensitivity of NSCLC cells to cisplatin-induced apoptosis by targeting c-Jun (16).

miR-383 is a tumor suppressor that plays important roles in multiple types of cancer, such as gastric cancer, prostate cancer and cervical cancer (17,18). A previous study reported that in the clinic, miR-383 was markedly downregulated in NSCLC carcinoma tissues, in a stage dependent manner, and low tumoral miR-383 expression was negatively correlated with the overall survival of patients with NSCLC (19). However, it is not clear why miRNA-383 is downregulated in lung adenocarcinoma tissues. Another study demonstrated that overexpression of miR-383 in NSCLC cells significantly decreased cell proliferation, migration and invasion through repression of endothelial PAS domain-containing protein 1 (20). However, the role of miR-383 in the survival of lung adenocarcinoma cells upon chemotherapy remains unknown, to the best of our knowledge. The aim of the present study was to determine the mechanism underlying miR-383 downregulation in lung adenocarcinoma tissues, and how miR-383 regulated the chemosensitivity of lung adenocarcinoma cells. The results suggested a novel diagnostic and prognostic biomarker for lung adenocarcinoma, which may highlight a potential therapeutic strategy for the clinical reversal of chemotherapy resistance in lung adenocarcinoma.

Materials and methods

Plasmids. Human miR-383-encoding DNA was subcloned into pLKO.1-TRC cloning vector (plasmid #10878; Addgene, Inc.) between *Age*I and *Eco*RI restriction sites to construct the miR-383 overexpression vector pLKO.1-miR-383. The empty pLKO.1-TRC cloning vector served as a control. Human miR-383-encoding DNA was amplified by PCR using genomic DNA extracted from A549 cells. Human RBM24-encoding DNA was cloned into pLenti-CMV-GFP-Puro (plasmid #17448, Addgene) between *Bam*HI and *Sal*I restriction sites to form the overexpression vector pLenti-CMV-RBM24. Human RBM24 DNA was also cloned into pCDNA3.1 between *Bam*HI and *Eco*RI to form the overexpression vector pCDNA3.1-RBM24. Human RBM24-encoding DNA was amplified by PCR using cDNA prepared from A549 cells. TargetScan (targetscan.org) and miRanda (microran.org) were used to predict the potential target untranslated regions (UTRs) of miR-383. A 40-bp annealed DNA fragment identical to part of the RBM24-3'UTR containing the predicted miR-383-binding site (TCTGATC) was inserted into *Pme*I and *Xba*I sites of pMIR-GLO, generating pMIR-3'UTR/WT. pMIR-3'UTR/Mut, served as the control, and was generated by introducing the same annealed DNA fragment with mutations in the miR-383 seed region (CGCCTCG). Primers used for PCR and cloning are listed in Table I.

Cell culture and transfection. Human lung epithelial cells NuLi-1, human bronchial epithelial cells HBE (CVCL_0287, Cellosaurus), Human lung cancer cell lines A549, H1299, H1650, H460 and A549/CDDP, a cisplatin resistant A549 cell line that was established in our previous study (21), were cultured in RPMI-1640 medium (Cellgro; Corning, Inc.) supplemented with 10% FBS (HyClone; Cytiva), 100 U/ml penicillin, and 100 mg/ml streptomycin (Cellgro; Corning, Inc.) at 37°C with 5% CO_2 in a humidified incubator. For stable ectopic overexpression of miR-383 and RBM24, a

2nd generation lentiviral system was used for lentivirus packaging. Briefly, 5 µg of each pLKO.1-miR-383, pLKO.1-TRC cloning, pLenti-CMV-GFP-Puro or pLenti-CMV-RBM24 vector as well as lentiviral helper vectors pCMV-VSV-G (3.75 µg, Addgene plasmid, cat. no. 8454) and pCMV-dR8.2 dvpr (1.25 µg, Addgene plasmid, cat. no. 8455) were co-transfected into 293T cells for 72 h, after which the lentiviral particles were harvested. Cells were infected with lentiviral particles at a multiplicity of infection of 10 for 24 h and selected with 2 µg/ml puromycin (Sigma-Aldrich; Merck KGaA) for 1 week to establish A549-Le/miR-383, A549-Le/RBM24 and A549/CDDP-Le/miR-383 cells. Empty lentiviral particles infected and stable selected A549-Le/control or A549/CDDP-Le/control cells served as controls. Plasmids were transfected using Effectene Transfection Reagent (Qiagen GmbH) according to the manufacturer's protocol. Human RBM24 small interfering RNA (RBM24 siRNA), nonsense control siRNA (siRNA NC), miR-383 inhibitor and nonsense control miRNA (miRNA NC) were synthesized by Shanghai GenePharma, Co., Ltd. The sequences are listed in Table I. HiPerFect Transfection Reagent (Qiagen GmbH) was used to transfect siRNA or miRNA into cells according to the manufacturer instructions. Briefly, 100 pmol of each siRNA or miRNA were transfected into one well of the 6-well plate. Transfected cells were then incubated 2 days at 37°C before further analysis.

Patient samples. Lung adenocarcinoma tissues and their corresponding non-cancerous tissues were randomly collected from 93 patients, including 37 males and 56 females, (age range, 30-84; median age, 62 years) who underwent surgery at the Southwest Hospital of the Army Medical University (Chongqing, China) between July 2008 and June 2010. The subjects were diagnosed with lung adenocarcinoma based on clinical manifestations, medical history and pathological results, and had no history of other malignancies or relevant antitumor treatments before the surgical resection. The histopathological classification was based on the standard formulated by World Health Organization in 1999 (22), and staging was based on the criteria developed by the International Union Against Cancer in 2009 (23). Each pair of samples were split into two halves. All samples were frozen in liquid nitrogen within 10 min after surgery and stored at -80°C until required for analysis. Procedures for the collection of human samples and their use for tissue arrays and gene expression studies were approved by the Ethical Committee of the Army Medical University (Chongqing, China). Signed informed consent forms were obtained from all patients prior to study participation.

Reverse transcription-quantitative (RT-q)PCR. Total RNA from cells, tumor tissues and paired adjacent non-tumor tissues were extracted using the QIAshredder and RNeasy kit (Qiagen GmbH). Accordingly, 1 mg RNA was reverse-transcribed to cDNA using SuperScript™ III Reverse Transcriptase (Takara Bio, Inc.). PCR was performed using the Phusion reaction system according to the manufacturer's protocol (Thermo Fisher Scientific, Inc.). miR-383 cDNA was synthesized using Hairpin-it™ miRNA RT-PCR Quantitation kit (Shanghai GenePharma, Co., Ltd.) at 25°C for 30 min, 42°C for 30 min

Table I. Sequences of the PCR primers, annealing primers, siRNAs and miRNA inhibitors.

Gene	Sequence, 5'-3'	Restriction enzyme
miR-383		
Forward	AAAC<u>ACCGGT</u>CCTGCAATGTGTATTGTTTGAT	*Age*I
Reverse	CCGG<u>AATTC</u>ATGGATACCCAAGGTCTCATGA	*Eco*RI
RBM24		
Forward	CGC<u>GGATCC</u>ATGCACACGACCCAGAAGGACA	*Bam*HI
Reverse 1	ACGC<u>GTCGAC</u>GGTCTATTGCATTCGGTCTGTCTGC	*Sal*I
Reverse 2	CCGG<u>AATTC</u>GGTCTATTGCATTCGGTCTGTCTGC	*Eco*RI
RBM24-3'UTR		
Forward	AAACTAGCGGCCGCAGACCAGCCATCTGATCAAA GTTGAATTGTT	-
Reverse	CTAGAACAATTCAACTTTGATCAGATGGCTGGTCT GCGGCCGCTAGTTT	-
Mut RBM24-3'UTR		
Forward	AAACTAGCGGCCGCAGACCAGCCA**CGCCTCG**AA AGTTGAATTGTT	-
Reverse	CTAGAACAATTCAACTTT**CGAGGCG**TGGCTGGTC TGCGGCCGCTAGTTT	-
RBM24 siRNA	GGAUCAUGCAACCAGGUUUDTDT	-
siRNA NC	UUCUCCGAACGUGUCACGUDTDT	-
miR-383 inhibitor	AGCCACAAUCACCUUCUGAUCU	-
miRNA NC	CAGUACUUUUGUGUAGUACAA	-

Underlined, restriction sites; Bold, the mutant nucleotides of the 3'-UTR of RBM24. UTR, untranslated region; siRNA, small interfering RNA; miRNA/miR, microRNA; NC, non sense control.

and 85˚C for 5 min. qPCR was performed on a RT-PCR system (Bio-Rad Laboratories, Inc.). The thermocycling conditions were: 95˚C for 3 min; followed by 40 cycles of at 95˚C for 12 sec and 60˚C for 40 sec. The expression levels of miR-383 were normalized to U6. Detection of RBM24 mRNA was performed using a One Step SYBR PrimeScript™ RT-PCR kit II (Takara Bio, Inc.) and GAPDH expression was used as the loading control. The relative quantification of gene expression was determined using the comparative CT method ($2^{-\Delta\Delta Cq}$) (24). Primers used for RT-qPCR are listed in Table II.

Copy-number alteration (CNA) assays. The genomic DNA of each patient's tissue samples was extracted using the GenElute kit (cat. no. G1N70; Sigma-Aldrich; Merck KGaA) according to the manufacturer's protocol. The copy number was analyzed by using TaqMan Copy Number assays (Applied Biosystems; Thermo Fisher Scientific, Inc.) on the 7500 Fast Real Time PCR system. Briefly, the test assay (FAM™ labeled), the reference assay (VIC®-labeled) and the sample DNA were combined with the TaqMan® MasterMix, and then the standard TaqMan® Copy Number assay regimen was used to calculate the relative changes in copy number.

Cell viability and invasion assay. Cell viability was assessed using a Cell Counting Kit-8 (CCK-8) assay (cat. no. NQ646; Dojindo Molecular Technologies, Inc.). Briefly, $5x10^3$ cells/well were seeded into a 96-well plate and cultured overnight. Then, cells were treated with cisplatin for 48 h (for A549 cells the concentration of cisplatin used were: 0, 0.5, 1, 1.5, 2 or 4 µg/ml; for A549/CDDP cells the concentrations of cisplatin used were: 0, 2, 4, 8, 15 or 20 µg/ml). Next, 10 µl CCK-8 solution was added to each well and incubated in the dark for 2 h. The absorbance at 450 nm was measured using a microplate reader. The IC_{50} value was deduced according the cell viability curve. The 24-well Transwell plates with 8.0 µm pore size (cat. no. 3422, Corning) were used for invasion analysis. Briefly, Transwell inserts in which the upper chambers were precoated with Matrigel (cat. no. 356234; BD Biosciences) were seeded with $3x10^4$ cells in 200 µl serum-free medium, and 500 µl medium supplemented with 10% FBS was added to the lower chamber. Inserts were incubated at 37˚C with 5% CO_2 for 24 h, and the cells which had invaded to undersurface of the upper chamber were fixed with 4% paraformaldehyde for 30 min at room temperature and stained with 0.05% crystal violet for 15 min at room temperature. A total of 5 random fields of view from each chamber were imaged and counted under an inverted light microscope (magnification, x200; Olympus Corporation).

Tissue arrays. Arrays containing the 93 three tumor tissues and adjacent non-tumor tissues were generated using a tissue microarrayer (Leica Microsystems, Inc.). The streptavidin-biotin peroxidase complex method was used to immunohistochemically stain the paraffin embedded sections. The tissue arrays sections were deparaffinized, blocked using normal goat serum at 37˚C for 15 min (cat. no. ab7481; Abcam), and then incubated with anti-human RBM24 antibody (1:250;

Table II. Sequences of the primers used for reverse transcription-quantitative PCR.

Gene	Sequence, 5'-3'
miR-383	
Forward	AGATCAGAAGGTGATTGTGGCT
Reverse	TCTGACCAGGCAGTGCTGT
U6 snRNA	
Forward	CTCGCTTCGGCAGCACATATACT
Reverse	ACGCTTCACGAATTTGCGTGTC
RBM24	
Forward	CCAAGGATCATGCAACCAG
Reverse	GCAGGTATCCCGAAAGGTCT
GAPDH	
Forward	ATTCAACGGCACAGTCAAGG
Reverse	GCAGAAGGGGCGGAGATGA

RBM24, RNA binding motif protein 24; miR, microRNA.

cat. no. PA5-66881; Thermo Fisher Scientific, Inc.) at 4°C overnight. Signals were visualized using diaminobenzidine solution (Dako; Agilent Technologies, Inc.), following staining with hematoxylin staining solution for 5 min at room temperature (cat. no. C0107; Beyotime Institute of Biotechnology). Then, a graded semiquantitative scoring system was used to evaluate the expression of RBM24. The staining patterns were classified based on the percentage of area stained and the intensity of staining as follows: Negative, 0≤10%; sporadic, 11≤25%; focal, 26≤50%; or diffuse, ≥51%, and the staining intensity was classified as none, 0; weak, 1; strong, 2; or very strong, 3. An overall score was calculated by multiplying the intensity and positivity scores and stratified as follows: 0, negative; 1-3, weak staining; 4-6, moderate staining; and 7-9, strong staining (25). To analyze the clinical significance and prognosis, malignant samples with strong RBM24 staining were classified as high-expression, whereas low-expression was indicated by moderate staining and weak staining.

Immunoblotting. Cells were lysed in ice cold RIPA lysis buffer supplemented with a protease/phosphatase inhibitor cocktail (cat. no. KGP2100; Nanjing KeyGen Biotech Co., Ltd.). The protein concentration was determined using a Pierce BCA Protein Assay Kit (cat. no. 23227; Thermo Fisher Scientific, Inc.) according to the manufacturer's instructions. A total of 50 μg protein per sample was loaded on an 12% SDS gel, resolved using and transferred to a PVDF membrane (Invitrogen; Thermo Fisher Scientific, Inc.). After blocking with 5% skim milk, the PVDF membrane was incubated overnight at 4°C with the following primary antibodies: Anti-RBM24 (1:1,000; cat. no. PA5-66881; Thermo Fisher Scientific, Inc.), anti-phosphorylated-(p-)P65 (1:1,000; cat. no. 3033S; Cell Signaling Technology, Inc.), anti-P65 (1:1,000; cat. no. 8242S; Cell Signaling Technology, Inc.), anti-p-IκBα (1:1,000; cat. no. 2859S; Cell Signaling Technology, Inc.), anti-IκBα (1:1,000; cat. no. 4814S; Cell Signaling Technology, Inc.), anti-Bcl-2 (1:1,000; cat. no. 15071S; Cell Signaling Technology, Inc.), anti-Bcl-xL (1:1,000; cat. no. 2764S;

Cell Signaling Technology, Inc.) anti-cleaved caspase-3 (1:1,000; cat. no. 9661S; Cell Signaling Technology, Inc.) and anti-GAPDH (1:2,500; cat. no. PA5-116420; Thermo Fisher Scientific, Inc.). Then, the PVDF membranes were incubated with the corresponding horseradish peroxidase-conjugated Affinipure goat anti-rabbit IgG (1:5,000; cat. no. SA00001-1; ProteinTech Group, Inc. Group, Inc.) or goat anti-mouse IgG (1:5,000; cat. no. SA00001-2; ProteinTech Group, Inc. Group, Inc.) secondary antibodies. at room temperature for 1 h, and visualized using West Pico Super Signal chemiluminescent substrate (cat. no. 34095; Thermo Fisher Scientific, Inc.).

Dual-luciferase reporter assay. A549-Le/control and A549-Le/miR-383 cells were transfected with pMIR-Report luciferase vector containing the 3'-UTR of RBM24, including WT or Mut fragments, using Effectene Transfection Reagent. A total of 48 h after transfection, a Dual-Luciferase Reporter kit (Promega Corporation) was used to assay the luciferase activity according to the manufacturer's protocol. Each transfection was repeated three times.

Alkaline comet assay. Alkaline comet assays were performed to assess intra-strand and inter-strand crosslink formation using a Comet assay kit (cat. no. ab238544; Abcam) according to the manufacturer's protocol. Briefly, A549 cells stably overexpressing RBM24 and A549/CDDP cells stably overexpressing miR-383 were treated with their IC_{50} doses of cisplatin for 6 h. Then, cells were trypsinized and resuspended at $1x10^5$ cells/ml in ice-cold PBS (Mg^{2+} and Ca^{2+} free). Cell samples were combined with comet agarose and 75 μl of each sample was added onto the comet slide. After solidification, the slide was immersed in the pre-chilled lysis buffer for 1 h at 4°C and pre-chilled alkaline solution for a further 1 h at 4°C. Next, the slides were electrophoresed in TBE buffer for 30 min at 60 V at 4°C. After soaking in the pre-chilled DI H_2O three times (2 min/each), the slides were immersed in cold 70% ethanol for 5 min. Subsequently, they were air dried, and 100 μl/well diluted Vista Green DNA Dye was added and incubated at room temperature for 15 min. Epifluorescence microscopy (magnification, x200; Olympus Corporation) with a FITC filter was used to capture images of the cells, and the mean tail moment was calculated using Comet Score version 1.5 (TriTeK Corp.).

Generation of xenografts and drug treatment. miR-control and miR-383 tumor xenografts were established by subcutaneously inoculating $5x10^6$ cells (A549-Le/control and A549-Le/miR-383 cells resuspended in PBS at $5x10^7$ cells/ml) into 4-week-old male BALB/c nude mice in the right flank next to the hind limb (n=20 per group; 40 in total; average weight, 16 g). A total of 28 days later, xenograft tumors that were ~1.5 cm in length and diameter were selected for drug treatment (n=9 per group). The volume of each tumor was calculated according to the formula volume=$A^2B/2$, where A represents the length/diameter and B represents the short diameter. Selected mice were subjected to peritoneal injection of 4 mg/kg cisplatin once every week for 3 weeks. Every 6 days after initiation of treatment, the tumor volumes were measured. Then all mice were sacrificed to harvest the tumor tissues to perform immunohistochemistry assays. All

procedures for animal experiments were approved by the Committee on the Use and Care on Animals [Army Medical University (previously known as The Third Military Medical University), Chongqing, China] and performed in accordance with institutional guidelines. Mice were housed in a specific pathogen-free facility with temperature at 24±1°C, relative humidity at 40-60%, a 12:12 h light/dark cycle and free access to food and water. All animals received humane care according to the criteria outlined in the Guide for the Care and Use of Laboratory Animals prepared by the National Academy (26). At the end of the experiment, all animals were euthanized by CO_2 inhalation with a chamber volume displacement rate of 30% per minute (volume/min; performed between March and September 2020).

Statistical analysis. Survival curves were plotted using the Kaplan-Meier method, and the correlation between miR-383 or RBM24 expression and the overall survival of patients with NSCLC was estimated using a log-rank (Mantel-Cox) test. The comparison between two groups was determined using a paired Student's t-test, and differences between multiple groups were determined by ANOVA followed by a Tukey's post-hoc test of pairwise differences (Tukey Honest Significant Difference). The statistical analysis was performed using SPSS version 19.0 (IBM, Corp.), and data are presented as the mean ± the standard deviation. P<0.05 was considered to indicate a statistically significant difference. The relationship between RBM24 expression and miR-383 expression was evaluated using Spearman's rank correlation analysis.

Results

miRNA-383 expression is downregulated in patients with lung adenocarcinoma and this is associated with worse survival outcomes. miR-383 expression profiling was performed on a cohort of 93 patients with lung adenocarcinoma. Expression was analyzed and compared with the matching non-cancerous tissues by RT-qPCR. miR-383 expression was found to be significantly downregulated in 70% of lung adenocarcinoma cases (Fig. 1A). A total of 9.6% of lung adenocarcinoma cases showed no change in expression, whereas 20.4% of cases exhibited upregulated miR-383 expression. The average miR-383 expression in lung adenocarcinoma tissues was ~6-fold lower than that in non-cancerous tissues (P=0.017; Fig. 1B). miR-383 is located in a common region of loss of heterozygosity (LOH) at the chr8p22 locus within intron 3 of the Sarcoglycan ζ (SGCZ) gene (18). Next, the CNAs at this locus in this cohort (n=93) were analyzed, and it was found that ~44% of lung adenocarcinoma tissues exhibited heterozygous or homozygous loss at the miR-383 locus compared with the adjacent non-cancerous tissues (Fig. 1C). Additionally, the correlation between CNAs and miR-383 expression within this cohort was analyzed, and the results showed a positive correlation (r=0.4457, P<0.0001; Fig. 1D). In consideration of the universal downregulation of miR-383 expression in lung adenocarcinoma clinical specimens, analysis of miR-383 expression with the clinicopathological parameters was performed. The levels of miR-383 expression were stratified into high (no change and upregulation, ≥0.75; n=28) and low (downregulation, <0.75; n=65) expression groups relative to

matched noncancerous tissue. Kaplan-Meier survival analysis showed that patients with low miR-383 expression had significantly poorer survival outcomes (P=0.0029; Fig. 1E). Additionally, a low level of miR-383 expression in lung adenocarcinoma was significantly associated with a higher mortality rate (P=0.045), Tumor-Node-Metastasis stage (P=0.027) and metastasis (P=0.044) (Table III). These results suggested that low miR-383 expression may be involved in the progression of lung adenocarcinoma.

miRNA-383 sensitizes lung adenocarcinoma cells to cisplatin. The expression patterns of miR-383 in lung adenocarcinoma cell lines *in vitro* were assessed. Compared with the NuLi-1 and HBE cells, endogenous miR-383 expression in lung adenocarcinoma cell lines was significantly downregulated, including H1299, H1650, H460, A549 and A549/CDDP cells (Fig. 2A). Compared with the parental A549 cells, the expression of miR-383 in cisplatin-resistant counterparts (A549/CDDP cells) was further reduced. To study the function of miR-383, a miR-383 overexpression plasmid was created using the pLKO.1 vector (Fig. 2B). Using lentiviral infection and selection, miR-383 was overexpressed in A549 and A549/CDDP cells (Fig. 2C and D). Overexpression of miR-383 inhibited the proliferation, migration and invasion of A549 cells (Fig. S1). Cell viability analysis showed that the high expression of miR-383 significantly increased the sensitivity of cells to cisplatin; that is, the IC_{50} of A549 cells decreased from 2 to 1.3 μg/ml, whereas the IC_{50} of A549/CDDP decreased from 9 to 5.5 μg/ml (Fig. 2E and F). These results suggested that miR-383 was involved in cisplatin resistance in lung adenocarcinoma cells.

miRNA-383 modulates RBM24 expression in lung adenocarcinoma cells. To investigate how miR-383 affected the sensitivity of lung adenocarcinoma cells to cisplatin, TargetScan (targetscan.org) and miRanda (microran.org) were used, and they showed that that RBM24 was a predicted target of miR-383. According to bioinformatics analysis, the specific miR-383 binding site was located within the 3'UTR of RBM24 mRNA (Fig. 3A). To investigate whether miR-383 directly targets the 3'UTR of RBM24 mRNA, the wild-type (RBM24-3'UTR/WT) or mutant (RBM24-3'UTR/Mut) 3'UTR of RBM24 mRNA was inserted into the pMIR-REPORT vector for luciferase activity analysis (Fig. 3B). Using a dual luciferase reporter assay, it was shown that miR-383 stably overexpressing cells exhibited remarkably decreased luciferase activity in the 3'UTR/WT group, whereas no significant reduction was observed in the pMIR-control or 3'UTR/Mut group (Fig. 3C). Next, the mRNA expression patterns of RBM24 in the abovementioned lung adenocarcinoma cell lines was determined. Compared with the NuLi-1 and HBE cells, endogenous RBM24 mRNA expression was significantly upregulated in lung adenocarcinoma cell lines and further enhanced in cisplatin-resistant A549 cells (Fig. 3D). Analysis of the expression patterns of miR-383 and RBM24 mRNA revealed that miR-383 and RBM24 were inversely associated in these lung adenocarcinoma cell lines (Fig. 3E). Additionally, RBM24 mRNA expression profiling was performed on the patient cohort samples, and it was shown that RBM24 was significantly upregulated in 61.3% of lung adenocarcinoma cases (Fig. 3F).
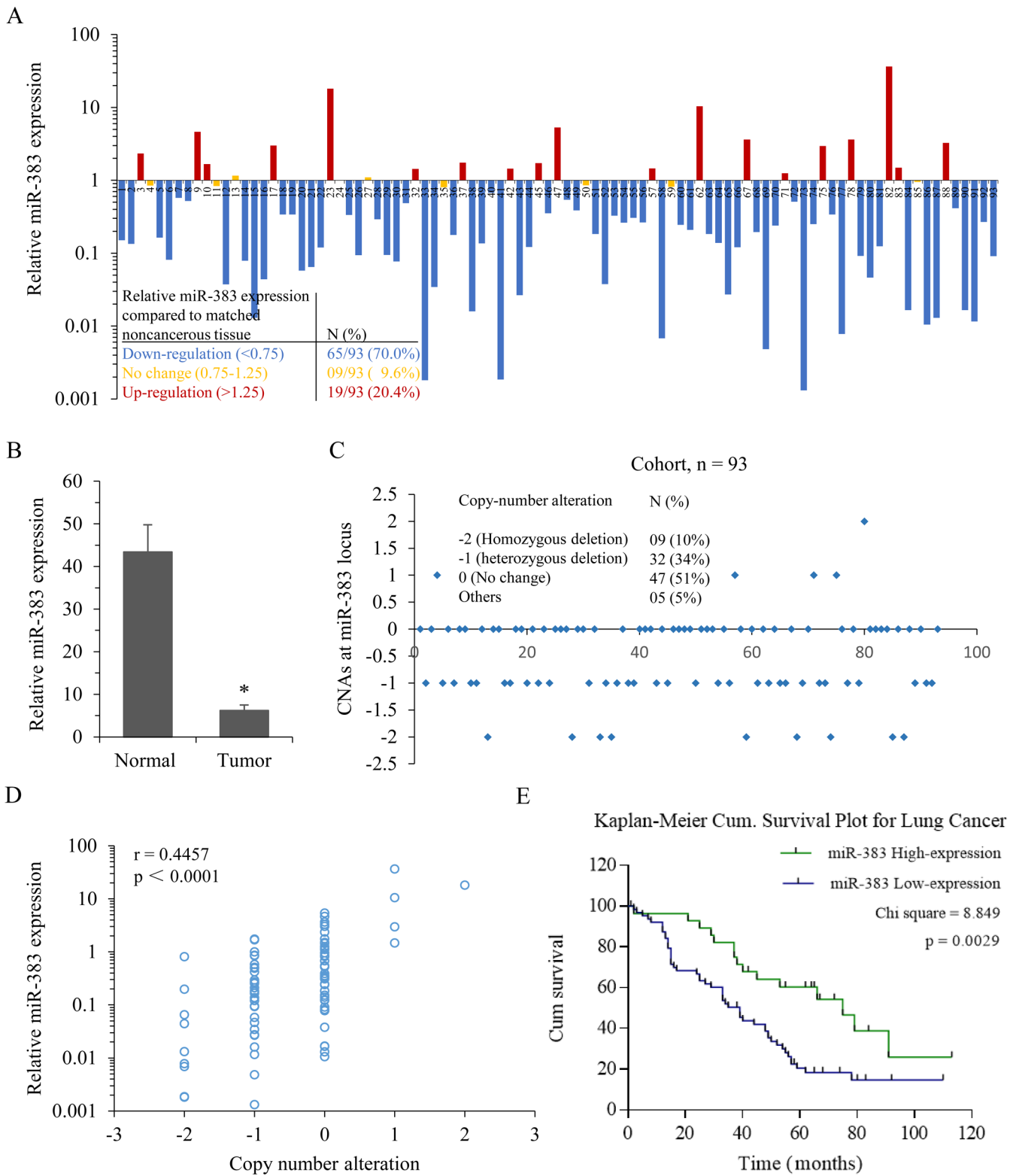
Figure 1. miR-383 downregulation in cancer cells is associated with a poorer prognosis in patients with lung adenocarcinoma. (A) miR-383 levels were quantified in lung adenocarcinoma samples and non-cancerous lung tissues. miR-383 expression was normalized to U6 and each non-cancerous lung tissue was used as a respective control (n=93). (B) miR-383 expression in tumor tissues and non-cancerous lung tissues of the cohort. Data are presented as the mean ± standard deviation. *P<0.05. (C) CNAs at the miR-383 locus in the lung adenocarcinoma tissues of the cohort. (D) Correlation between miR-383 expression and CNAs in the cohort. (E) Kaplan-Meier analysis of overall survival in the patients with lung adenocarcinoma according to the expression levels of miR-383 in lung cancer tissues; miR-383 high expression, n=28 and miR-383 low expression, n=65. miR, microRNA; CNA, copy number alteration; Cum, Cumulative.

A total of 16.1% of lung adenocarcinoma cases showed no change, and 22.6% of cases exhibited reduced RBM24 mRNA expression. Similar to what was observed in the lung adenocarcinoma cell lines, the levels of miR-383 and RBM24 mRNA

Table III. Relationship between miR-383 expression and of association with the clinicopathological characteristics of the 93 patients used in the present study.

Characteristic	Number of cases	miR-383 expression		P-value
		Low, n (%)	High (%)	
Sex				0.121
Male	37	22 (59.5)	15 (40.5)	
Female	56	43 (17.1)	13 (82.9)	
Age, years				0.247
≥60	50	38 (76.0)	12 (24.0)	
<60	43	27 (62.8)	16 (37.2)	
Death				0.045[a]
No	65	50 (76.9)	15 (23.1)	
Yes	28	15 (53.6)	13 (46.4)	
Tumor grading				0.381
1	19	11 (57.9)	08 (42.1)	
2	48	34 (70.8)	14 (29.2)	
3	26	20 (76.9)	06 (23.1)	
Tumor-Node-Metastasis stage				0.027[a]
Early (I/II)	42	24 (57.1)	18 (42.9)	
Advanced (III)	51	41 (80.4)	10 (19.6)	
Lymph node metastasis				0.044[a]
No	37	21 (56.8)	16 (43.2)	
Yes	56	44 (78.6)	12 (21.4)	

[a]$P<0.05$.

in the clinical specimens were inversely associated (Fig. 3G). Moreover, overexpression of miR-383 inhibited the expression of RBM24 in both parental A549 cells and A549/CDDP cells (Fig. S2A and B). Together, these results suggested an inverse association between RBM24 mRNA and miR-383 expression levels in lung adenocarcinoma cells.

RBM24 upregulation in lung cancer is correlated with a poorer prognosis. To further investigate whether aberrant RBM24 expression can be used to predict prognosis in patients with lung adenocarcinoma, a tissue array was generated using the tissue samples obtained from the cohort, and RBM24 expression was determined using immunohistochemistry. Representative images with strong, moderate and weak staining in the tumor tissue and non-cancerous samples are shown in Fig. 4A. Strong staining was observed in 52.7% of tumor samples, whereas moderate and weak staining were found in 31.2 and 16.1% of samples, respectively (Fig. 4B). In contrast, RBM24 expression was relatively lower in non-cancerous lung tissues. Strong positivity was found in only 20.4% of samples, whereas moderate and weak RBM24 expression was observed in 58.1 and 21.5% of tissues, respectively (Fig. 4C). Importantly, RBM24 upregulation was associated with shorter overall survival than RBM24 low expression (including moderate and weak staining) in patients (P=0.0061; Fig. 4D).

miRNA-383 negatively regulates RBM24 expression, resulting in increased cisplatin sensitivity of lung adenocarcinoma. Next, whether RBM24 could affect the sensitivity of lung adenocarcinoma cells to cisplatin was assessed. First, the expression of RBM24 in parental and cisplatin resistant A549 cells was determined, and the results showed that A549/CDDP cells demonstrated significantly increased expression of RBM24 (Fig. 5A). After knocking down RBM24 expression using siRNA (Fig. S2C), the IC$_{50}$ of A549/CDDP cells decreased from ~9 to ~3.5 μg/ml (Fig. 5B and C). In contrast, with stable overexpression of RBM24 in A549 cells, the IC$_{50}$ increased from 1.7 to ~3.0 μg/ml (Fig. 5D and E). In addition, neutralization of miR-383 using an inhibitor in A549 cells (Fig. S2D) increased the expression of RBM24 and enhanced tolerance to cisplatin, increasing the IC$_{50}$ from 1.6 to 2.8 μg/ml (Fig. 5F and G). Moreover, knockdown of RBM24 overcame the upregulation of RBM24 expression induced by neutralization of miR-383 and reduced the IC$_{50}$ to ~0.8 μg/ml (Fig. 5H and I). In addition, a comet assay demonstrated that overexpression of RBM24 inhibited the formation of DNA double-stranded breaks induced by treatment with an IC$_{50}$ dose cisplatin in A549 cells, whereas overexpression of miR-383 in A549/CDDP cells promoted their formation (Fig. 5J). Taken together, these data demonstrated that miR-383 downregulation may be responsible for the upregulation of RBM24, which partly contributed to the cisplatin resistance of lung adenocarcinoma cells.
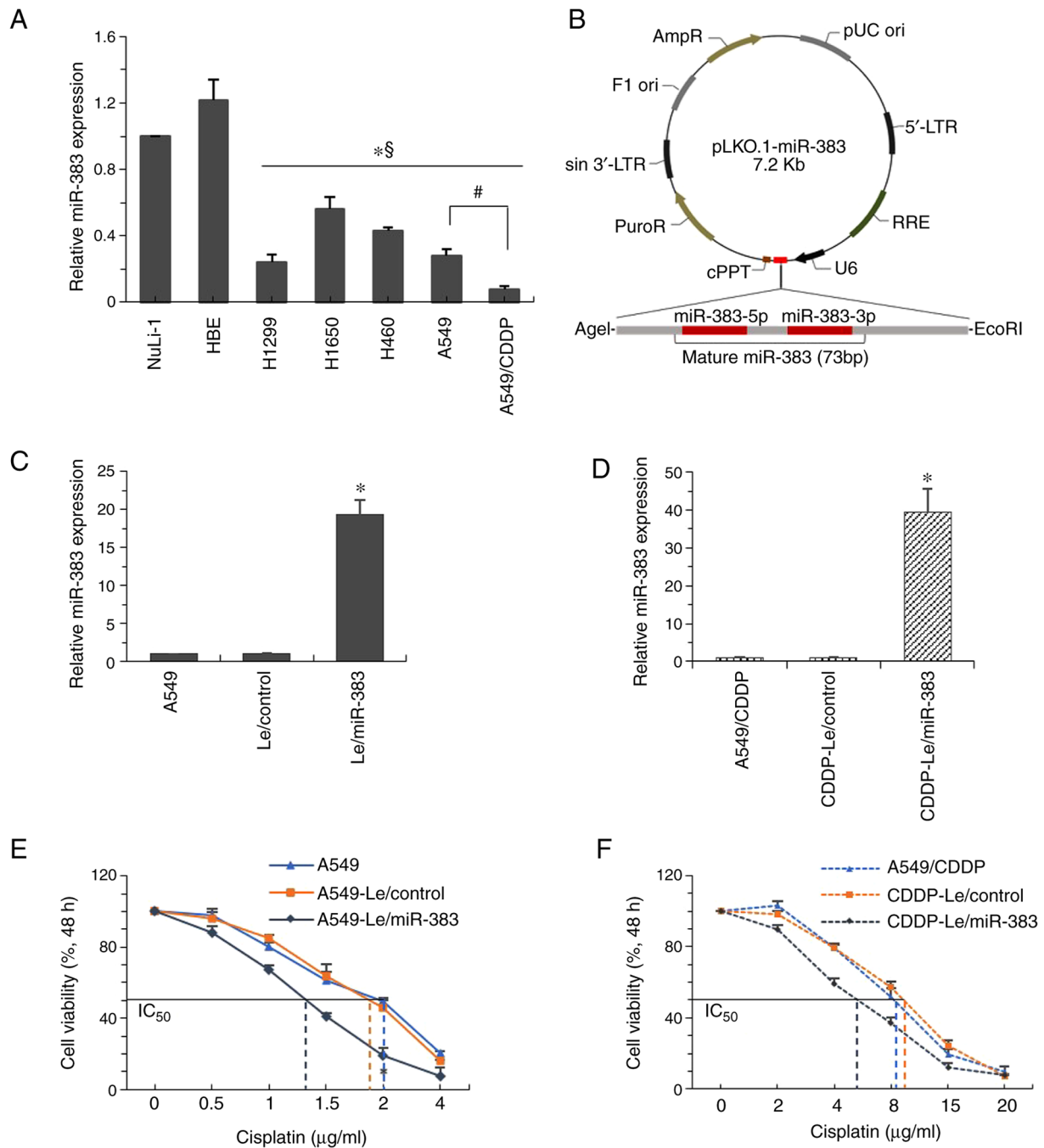
Figure 2. miR-383 sensitizes lung adenocarcinoma cells to cisplatin. (A) RT-qPCR was used to quantify the expression of miR-383 in the lung adenocarcinoma cell lines, H1299, H1650, H460, A549 and A549/CDDP, and then normalized to miR-383 expression in the normal human bronchial epithelium cell line, NuLi-1. *P<0.05 vs. NuLi-1; §P<0.05 vs. HBE cells; #P<0.05, A549/CDDP vs. A549 cells. (B) The vector for overexpression of miR-383. Mature miR-383-encoding DNA was directly inserted downstream of the U6 promoter to create the pLKO.1-miR-383 vector. (C) Expression of miR-383 was determined by RT-qPCR in A549-Le/miR-383 cells and A549-Le/control cells, and normalized to the expression in A549 cells. (D) miR-383 expression was determined by RT-qPCR in A549/CDDP-Le/miR-383 cells and A549/CDDP-Le/control cells, and normalized to the expression in A549/CDDP cells. *P<0.05. The effect of miR-383 overexpression on the viability of (E) A549 and (F) A549/CDDP cells after treatment with different concentrations of cisplatin for 48 h. Data are presented as the mean ± standard deviation of three sets of independent experiments. miR, microRNA; RT-qPCR, reverse transcription-quantitative PCR; Le, lentiviral vector; A549/CDDP, cisplatin-resistant A549 cells.

miRNA-383 suppresses the activation of RBM24 mediated NF-κB signaling. Next, the effect of miR-383 on the activation of NF-κB signaling was investigated. Western blot analysis demonstrated that in both A549 and A549/CDDP cells, restoration of miR-383 significantly decreased the Ser536-phosphorylation of p65 and Ser32-phosphorylation of IκBα. Moreover, consistent with the expression of RBM24, the anti-apoptosis-related proteins Bcl-2 and Bcl-xL were both downregulated (Fig. 6A). Using siRNA to knockdown RBM24 expression in A549/CDDP cells, similar results were observed. The levels of phosphorylated p65 and IκBα, as well as Bcl-2 and Bcl-xL expression were also decreased (Fig. 6B). Given that RBM24 was identified as the direct target of miR-383, whether miR-383-mediated inactivation of NF-κB was associated with
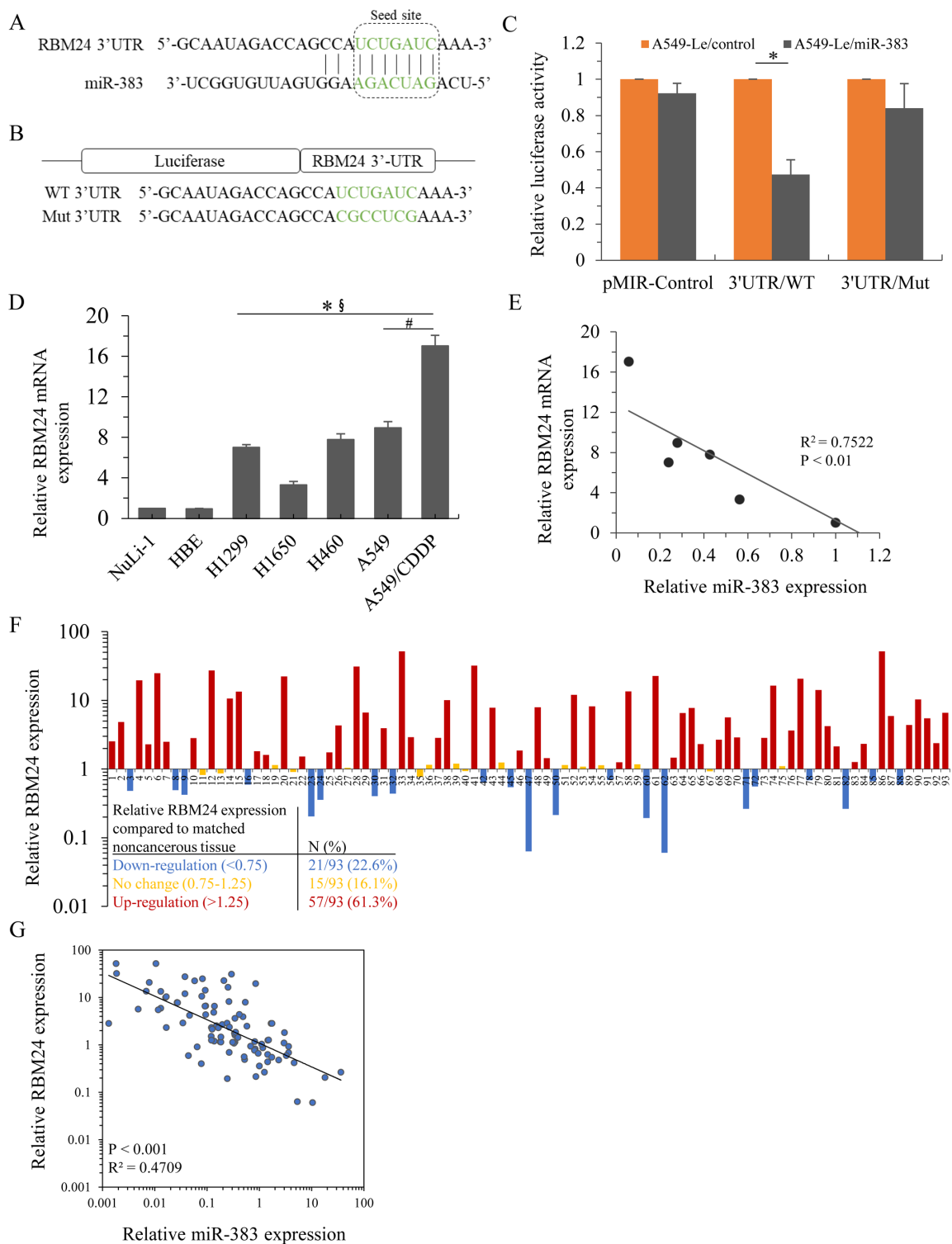
Figure 3. miR-383 modulates RBM24 expression in lung adenocarcinoma cells. (A) The 3'-UTR of RBM24 contains one predicted miR-383 binding site. (B) The WT or Mut RBM24 mRNA 3'-UTR sequence was subcloned into the pMIR-GLO luciferase reporter. (C) The WT or Mut reporter plasmids were transfected into A549-Le/control or A549-Le/miR-383 cells. Luciferase activity is presented relative to the normalized luciferase activity in the A549-Le/control group. (D) mRNA expression analysis of RBM24 in lung adenocarcinoma and normal human bronchial epithelium cell lines. NuLi-1 cells severed as the control. *$P<0.05$ vs. NuLi-1; §$P<0.05$ vs. HBE cells; #$P<0.05$, A549/CDDP vs. A549. Data are presented as the mean ± standard deviation of three independent experiments. (E) A statistically significant negative correlation was identified between miR-383 and RBMA24 expression levels in lung cancer cell lines. $P<0.01$. (F) RBM24 mRNA levels were quantified in lung adenocarcinoma samples and non-cancerous lung tissues. RBM24 expression was normalized to GAPDH, and each respective non-cancerous lung tissue was used as a control. (G) Correlation between the expression levels of RBM24 and miR-383 in clinical lung adenocarcinoma tissues. $P<0.001$. RBM24, RNA binding motif protein 24; miR, microRNA; 3'-UTR, 3'-untranslated region; Le, lentiviral vector.

downregulation of RBM24 was next assessed. Rescue experiments showed that overexpression of RBM24 restored the phosphorylation of p65 and IκBα by increasing the expression of Bcl-2 and Bcl-xL in miR-383-overexpressing A549/CDDP cells (Fig. 6C). In addition, the results also demonstrated that overexpression of RBM24 in A549 cells partially inhibited the
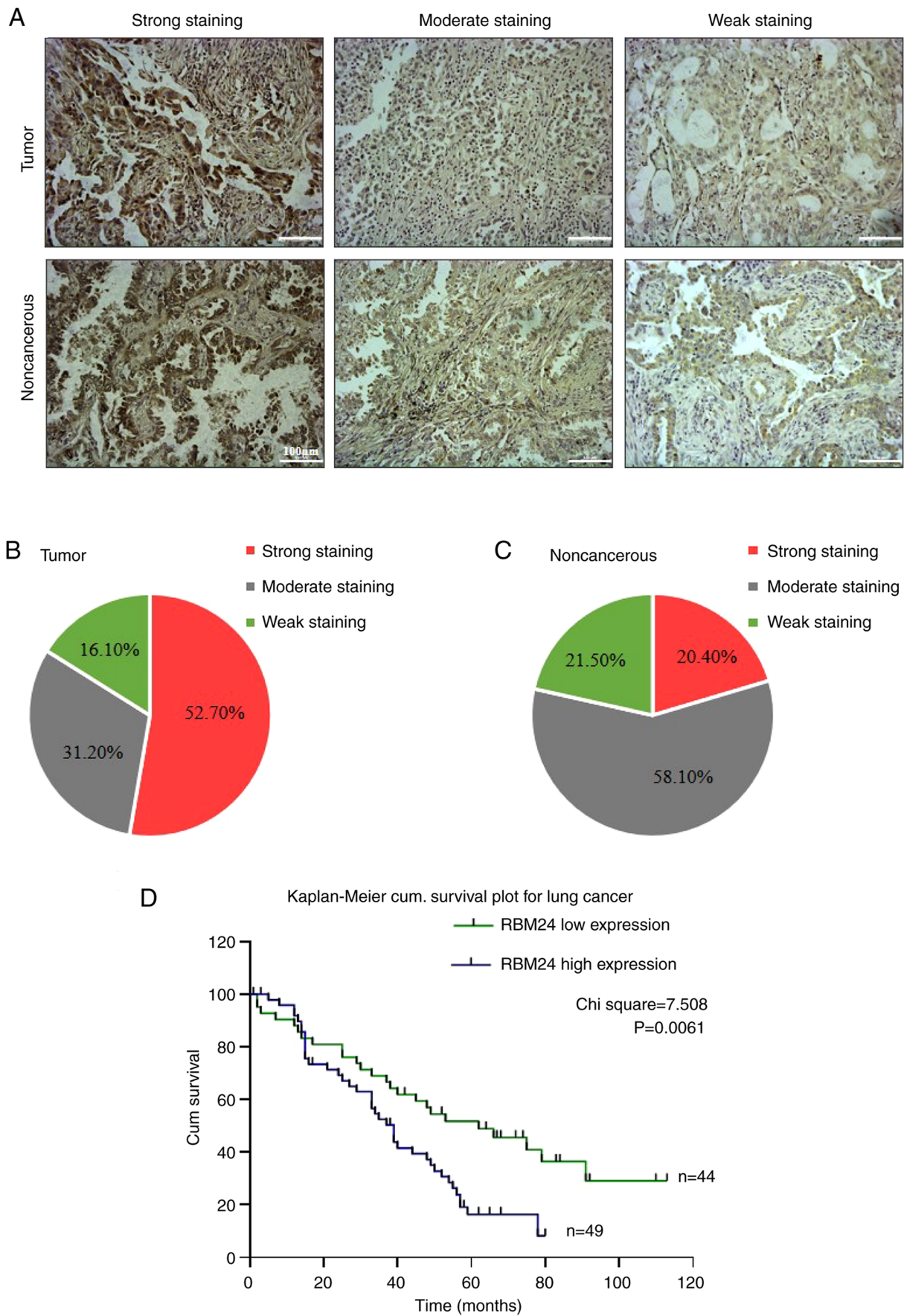
Figure 4. RBM24 upregulation in cancer cells is associated with a worse prognosis in patients with lung cancer. (A) Representative images showing strong, moderate and weak staining of RBM24 in lung cancer tissues and their corresponding non-cancerous lung tissues using an immunohistochemistry tissue array. Magnification, x100; scale bar, 100 μm. (B and C) Pie charts showing the percentage of (B) lung cancer samples classed as showing strong, moderate or weak RBM24 expression and (C) the corresponding non-cancerous lung tissues. (D) Kaplan-Meier analysis of overall survival in patients with lung cancer based on the expression of RBM24 protein in lung cancer tissues; P=0.0061. RBM24, RNA binding motif protein 24; Cum, cumulative.
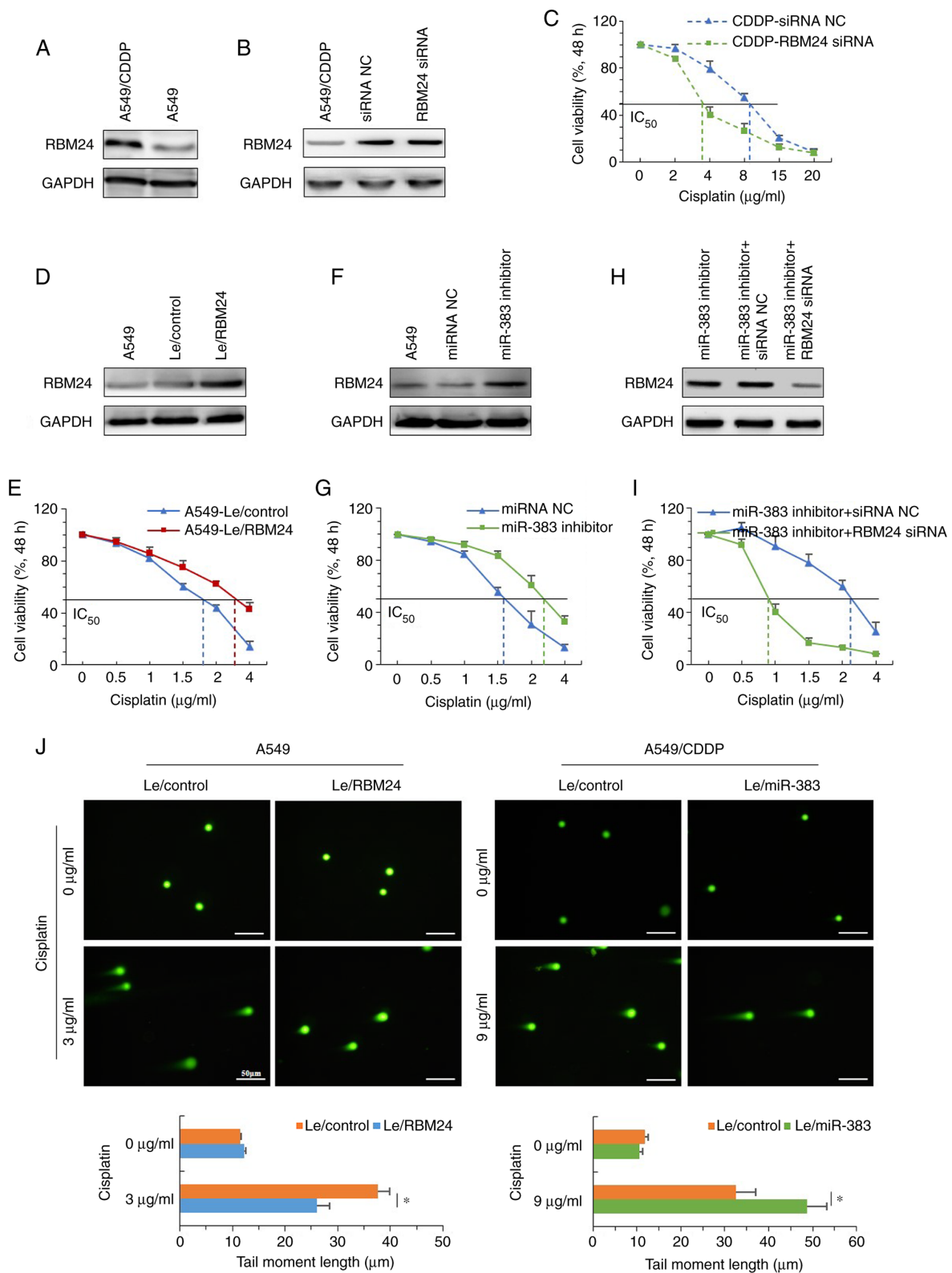
Figure 5. miR-383 enhances the sensitivity of lung adenocarcinoma cells to cisplatin through negative regulation of RBM24. (A) Protein expression levels of RBM24 were determined by immunoblotting in A549/CDDP and parental A549 cells. (B) A549/CDDP cells were transfected with siRNA NC or RBMA24 siRNA for 48 h, and RBM24 expression as assessed using western blotting. (C) Effect of RBM24 knockdown on the viability of A549/CDDP cells after treatment with different concentrations of cisplatin for 48 h. (D) Western blotting was used to determine the expression of RBM24 in A549 cells stably overexpressing RBM24 cells; uninfected and control lentivirus-infected A549 cells served as controls. (E) Effect of stable overexpression of RBM24 on the viability of A549 cells after treatment with different concentrations of cisplatin for 48 h. (F) A549 cells were transfected with miRNA NC or miR-383 inhibitor for 48 h, and RBM24 expression was assessed using western blotting. (G) Effect of miR-383 knockdown on the viability of A549 cells after treatment with different concentrations of cisplatin for 48 h. (H) A549 cells were co-transfected with miR-383 inhibitor and either RBM24 siRNA or siRNA NC for 48 h, and RBM24 expression was assessed by western blotting. (I) Effect of miR-383 and RBM24 knockdown on the viability of A549 cells after treatment with different concentrations of cisplatin for 48 h. (J) Representative images showing detectable comet tails visualized under a fluorescence microscope. Magnification, x200; scale bar, 50 μm. Data are presented as the mean ± standard deviation of three independent experiments. *P<0.05. miR, microRNA; RBM24, RNA binding motif protein 24; A549/CDDP, cisplatin-resistant A549 cells; siRNA, small interfering RNA; NC, nonsense control; miR/miRNA, microRNA.
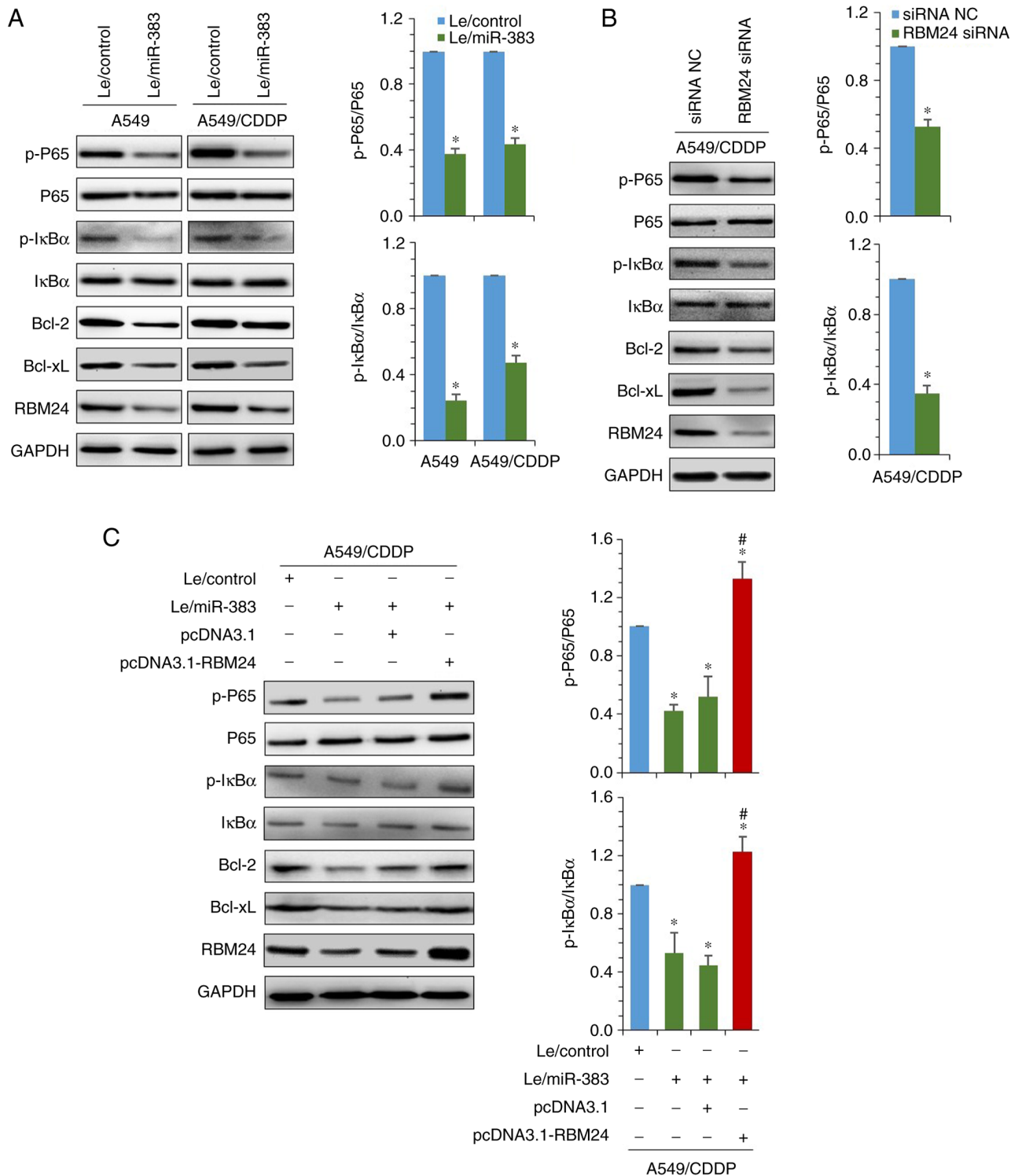
Figure 6. miR-383 inhibits RBM24-mediated NF-κB signaling activation. (A) Immunoblotting was used to detect the expression of NF-κB signaling regulatory factors and downstream target genes in A549 and A549/CDPP cells stably overexpressing miR-383 (left panel). Ratio of phosphorylated p65 and IκBα to total expression of p65 and IκBα (right panels). (B) RBM24 expression was knocked down using siRNA in A549/CDDP cells, and expression of the indicated proteins was detected by western blotting (left panel). Ratio of phosphorylated p65 and IκBα to total expression of p65 and IκBα (right panels). (C) Immunoblotting was used to detect the effect of transient overexpression of RBM24 on the expression of the indicated proteins in A549/CDDP cells following restoration of miR-383 expression (left panel). Ratio of phosphorylated p65 and IκBα to total p65 and IκBα expression (right panels). *P<0.05 vs. A549/CDDP-Le/control; #P<0.05, pCDNA3.1-RBM24 group vs. pCDNA3.1 group. Data are presented as the mean ± standard deviation of three independent experiments. miR, microRNA; RBM24, RNA binding motif protein 24; A549/CDDP, cisplatin-resistant A549 cells; NF-κB, nuclear factor κB; IκBα, inhibitor α of NF-κB; p-, phosphorylated; Le, lentiviral vector; Bcl-2, B-cell lymphoma-2; Bcl-xL, B-cell lymphoma-xL.

activation of caspase-3 (cleaved caspase-3) that were induced by 3 µg/ml cisplatin. However, 3 µg/ml cisplatin could not induce the activation of caspase-3 in A549/CDDP Le-control cells, whereas the expression of RBM24 was significantly inhibited in miR-383 overexpressing A549/CDDP cells, and the quantity of active caspase-3 induced by 3 µg/ml cisplatin
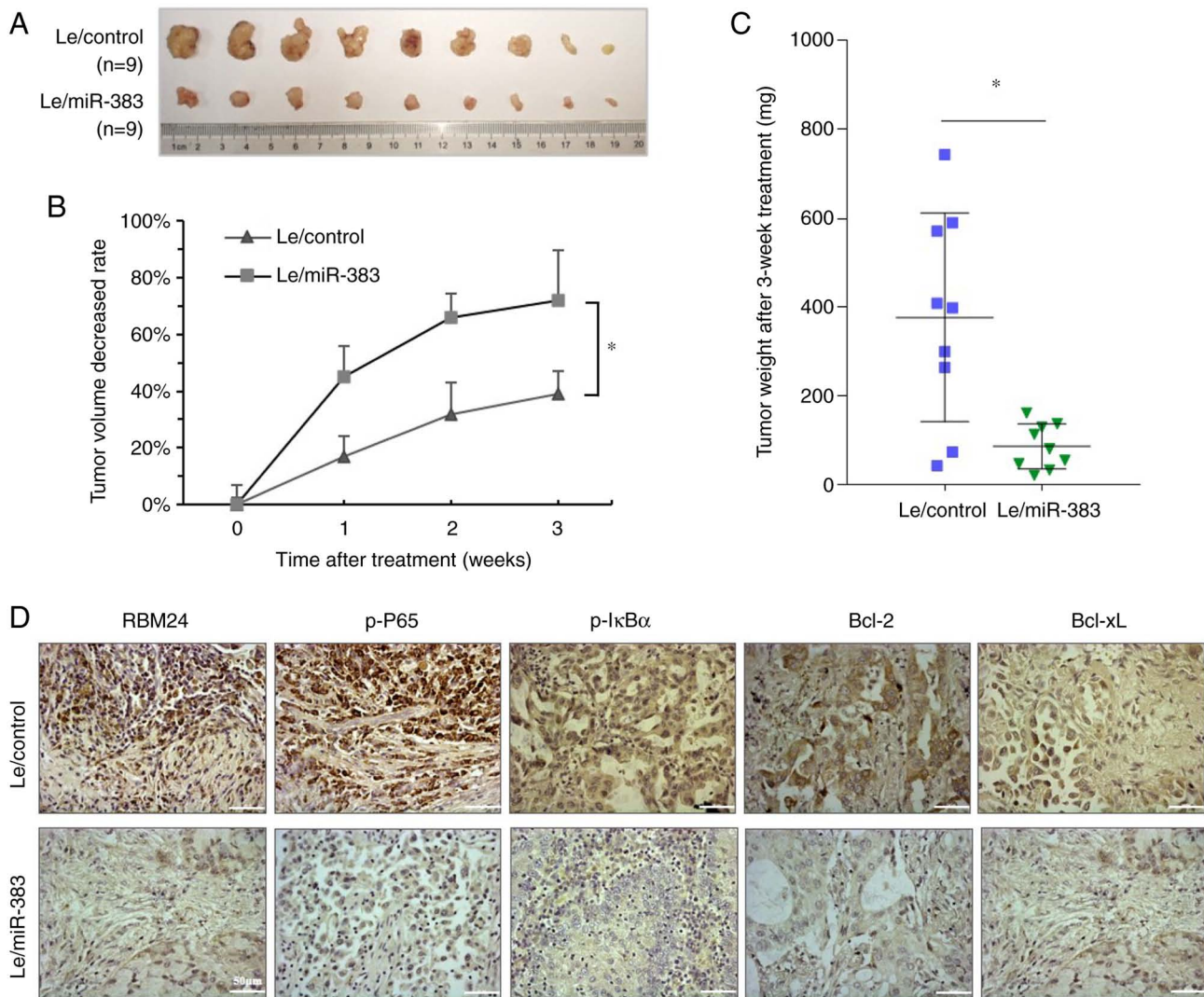
Figure 7. miR-383 enhances the cisplatin sensitivity of lung adenocarcinoma cells *in vivo*. (A) Tumor sizes of the Le-control and Le-miR-383 groups after 3 weeks of treatment with cisplatin. n=9. (B) Average rate of reduction of tumor volume in the indicated groups. *P<0.05. (C) Scatter plot showing the weight of tumors and horizontal lines indicate the average values. *P<0.01. (D) Representative images showing immunohistochemical staining analysis of the expression of the indicated genes. Magnification, x100; scale bar, 50 μm. miR, microRNA; A549/CDDP, cisplatin-resistant A549 cells; Le, lentiviral vector; p-, phosphorylated; RBM24, RNA binding motif protein 24.

was significantly increased (Fig. S3). Taken together, these findings suggest that targeting RBM24 was involved in the inhibition of NF-κB signaling by miR-383.

miR-383 enhances the cisplatin sensitivity of lung adeno-carcinoma cells in vivo. The role of miR-383 in the cisplatin sensitivity of lung adenocarcinoma cells was also investigated in an animal model. Xenograft tumors (n=9) of the A549/Le-miR-383 and A549/Le-control groups ~1.5 cm in length and diameter were selected for cisplatin treatment. After 3 weeks of treatment, tumors in the Le-miR-383 group were significantly smaller than those in the Le-control group (Fig. 7A). The average tumor volume gradually decreased after treatment in both groups, whereas the average tumor volume reduction rates of the Le-miR-383 group were significantly higher than those of the Le-control group (Fig. 7B). Additionally, the average weight of tumors was significantly lower in the Le-miR-383 group than in the Le-control group (Fig. 7C). Immunohistochemical staining revealed that in

the Le-miR-383 group, the expression of RBM24, p-P65 and p-IκBα, as well as the downstream Bcl-2 and Bcl-xL was suppressed compared with that in the Le-control group (Fig. 7D). These data suggested that miR-383-targeted RBM24 enhanced the sensitivity of lung adenocarcinoma cells to chemotherapeutics.

Discussion

Resistance to chemotherapeutic drugs is a difficult problem in antitumor research worldwide. It has been reported that >85% of patients with lung cancer treatment failure exhibit drug resistance (27). Therefore, research on the mechanism of lung cancer drug resistance, the identification of new antitumor targets and the development of new antitumor drugs have always been the focus of attention. miRNAs are a relatively more recent and important discovery in the field of RNA biology. There are >2,500 miRNAs expressed in the human body, and 60% of human genes may be regulated by them (28).
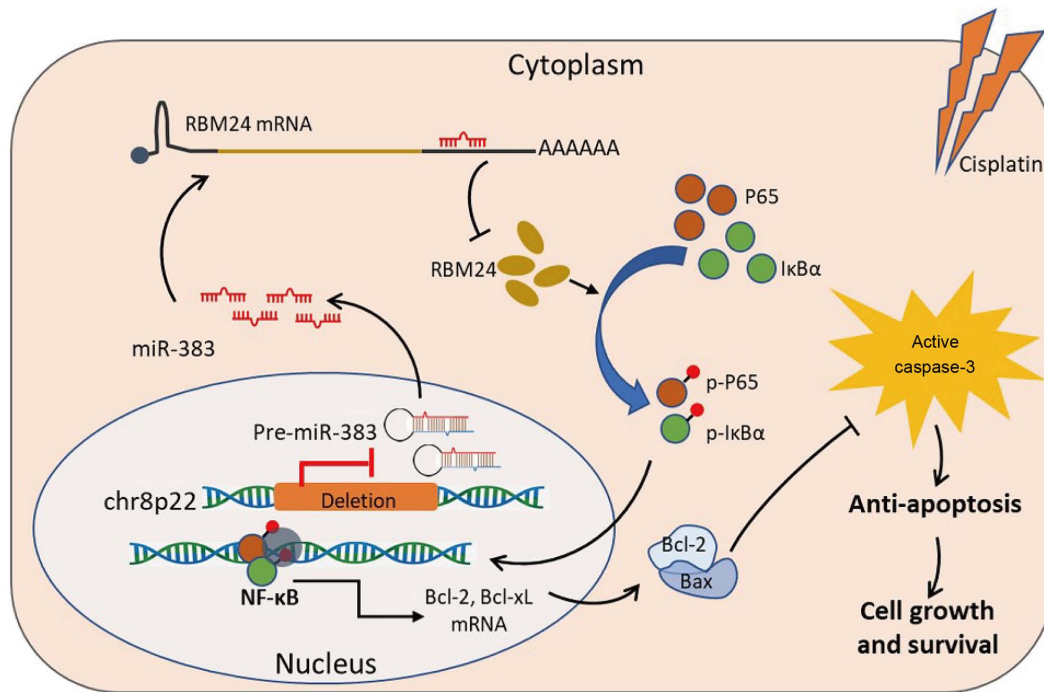
Figure 8. Model showing how miR-383 defects induce the expression of RBM24 to mediate chemotherapy resistance in lung adenocarcinoma cells. RBM24, RNA binding motif protein 24; miR, microRNA; p-, phosphorylated; NF-κB, nuclear factor κB; IκBα, inhibitor α of NF-κB; Bcl-2, B-cell lymphoma-2; Bcl-xL, B-cell lymphoma-xL.

These target genes are involved in a series of biological processes, such as individual development, cell differentiation, proliferation and apoptosis (29). Therefore, miRNAs serve important roles in the generation and development of human diseases, such as tumors and metabolic disorders. However, the roles and mechanisms in tumor drug resistance remain unclear.

miR-383 serves important roles in the progression of multiple tumors (30,31). The present study found that the expression of miR-383 in lung adenocarcinoma samples was reduced and related to the poor prognosis of patients. This conclusion is consistent with the results of previous studies assessing the same miRNA and type of cancer (32,33). Restoration of miR-383 inhibited the proliferation, migration and invasion of A549 cells. However, for the first time, the present study demonstrated that restoration of miR-383 expression promoted the cisplatin sensitivity of lung adeno-carcinoma cells. miR-383 promoted cisplatin sensitivity by interacting with the 3'-UTR of RBM24 mRNA to negatively regulate RBM24. Thus, these results highlight the potential of miR-383 and RBM24 as biomarkers for the early diagnosis and prognosis of lung adenocarcinoma.

The host gene SGCZ of miR-383 is located on chr8p22 (34). It has been reported that a common region of LOH at the chr8p22 locus is related to breast cancer and prostate cancer (18,35), and the present study also confirmed that the low expression of miR-383 in lung adenocarcinoma tissues was related to the deletion of this locus. In addition, miR-383 was shown to inhibit the activation of the NF-κB signaling pathway in the present study. Therefore, it was speculated that the abnormal activation of the NF-κB signaling pathway caused by the deletion of miR-383 may be partly responsible

for the natural resistance of certain lung adenocarcinoma cells to chemotherapy.

Mechanistically, overexpression of miR-383 inhibited the activation of NF-κB signaling in both A549 and A549/CDDP cells. NF-κB is a key modulator of apoptosis in cancer cells, which functions by regulating antiapoptotic-related genes, such as Bcl-2 and Bcl-xL (36). p65 is phosphorylated at multiple sites, and Ser536-phosphorylation enhances p65 transactivation potential (37). Chen *et al* (38) reported that IκBα-S32 and p65-S536 phosphorylation promoted the expression of Bcl-2. Bravo-Cuellar *et al* (39) reported that pentoxifylline and the proteasome inhibitor MG132 decreased the p65-S536 phosphorylation and the expression of Bcl-2 and Bcl-xL, inducing apoptosis in human leukemia U937 cells. The results of the present study also showed that overexpression of miR-383 led to a decrease in Bcl-2 and Bcl-xL expression in both A549 and A659/CDDP cells, along with a reduction in Ser536-phosphorylation of p65 and Ser32-phosphorylation of IκBα. However, the total expression of p65 and IκBα was not affected by miR-383. Further analysis showed that miR-383-mediated inactivation of NF-κB was due to the downregulation of RBM24. RBM24 is a member of the RNA binding protein family, and has a conserved RNA recognition motif at its N-terminus, which is mainly used as a post-transcriptional regulator to regulate RNA metabolism, and plays an important role in gene expression (40). A previous study showed that RBM24 inhibits the progression of nasopharyngeal carcinoma by upregulating miR-25 to target the metastasis associated with lung adeno-carcinoma transcript 1 (41). However, the present study found that RBM24 is highly expressed in lung adenocarcinoma and is positively correlated with the poor prognosis of patients.

The reason why the results of these studies are opposite may be due to differences in the biological function of RBM24 in different tissues/types of cancer. To the best of our knowledge, there are no studies assessing the correlation between RBM24 and tumorigenesis. It is necessary to further study the biological functions of RBM24 in different types of tumors. Studies have shown that RBM24 negatively regulates the expression of p53 and p63 by binding to specific regions of their mRNA, suggesting that RBM24 may negatively regulate the p53-mediated apoptosis pathway (42,43). The present study also showed that RBM24 can activate the NF-κB signaling pathway to promote the expression of downstream anti-apoptotic genes, including Bcl-2 and Bcl-xL. Therefore, it is hypothesized that the abnormally high expression of RBM24 mediates the cisplatin insensitivity of lung adenocarcinoma through multiple pathways. It is worth mentioning that RBM24 only changed the amount of phosphorylated p65 and IκBα, not the total expression. It is suggested that part of the reason is that RBM24 may affect the phosphorylation levels in cells through post-transcriptional regulation of the expression of certain kinases. Therefore, the exact mechanism by which RBM24 regulates the NF-κB signaling pathway needs further study.

In conclusion, the results of the present study demonstrated that chr8p22 loss resulted in defective expression of miR-383 in lung adenocarcinoma cells, leading to the upregulation of RBM24, which activates NF-κB signaling and causes the upregulation of downstream anti-apoptosis-related proteins, thus improving the tolerance of tumor cells to chemotherapy (Fig. 8). Restoration of miR-383 or interference of RBM24 may provide potential therapeutic approaches for reversing the chemotherapy resistance of lung adenocarcinoma.

Acknowledgements

Funding

Availability of data and materials

All data generated and/or analyzed during the present study are included in this published article.

Authors' contributions

YL and HW designed and conceived the study. BH and CW performed the experiments. WS and YQ collated and analyzed the clinicopathological data, and drafted the manuscript. JL, ZL and TJ performed the statistical analysis and data interpretation. All authors have read and approved the final manuscript. YL, BH and JL confirm the authenticity of all the raw data.

Ethics approval and consent to participate

The study protocol was approved by the Ethics Committee of the First Affiliated Hospital of the Army Medical University (previously known as Third Military Medical University), PLA (2015; Chongqing, China). Procedures for the collection of human samples, and their use for tissue arrays and gene expression studies were approved by the Ethical Committee of the Army Medical University (Chongqing, China). All patients signed an informed consent form and volunteered to participate in this study.

Patient consent for publication

Not applicable.

Competing interests

The authors declare that they have no competing interests.

References

1. Schwartz AG and Cote ML: Epidemiology of lung cancer. Adv Exp Med Biol 893: 21-41, 2016.
2. Siegel RL, Miller KD and Jemal A: Cancer statistics, 2020. CA Cancer J Clin 70: 7-30, 2020.
3. Miller KD, Nogueira L, Mariotto AB, Rowland JH, Yabroff KR, Alfano CM, Jemal A, Kramer JL and Siegel RL: Cancer treatment and survivorship statistics, 2019. CA Cancer J Clin 69: 363-385, 2019.
4. Xiong Y, Huang BY and Yin JY: Pharmacogenomics of platinum-based chemotherapy in non-small cell lung cancer: Focusing on DNA repair systems. Med Oncol 34: 48, 2017.
5. Denisenko TV, Budkevich IN and Zhivotovsky B: Cell death-based treatment of lung adenocarcinoma. Cell Death Dis 9: 117, 2018.
6. Zhao J, Xu T, Wang F, Cai W and Chen L: miR-493-5p suppresses hepatocellular carcinoma cell proliferation through targeting GP73. Biomed Pharmacother 90: 744-751, 2017.
7. Yu X and Li Z: MicroRNA expression and its implications for diagnosis and therapy of tongue squamous cell carcinoma. J Cell Mol Med 20: 10-16, 2016.
8. Gao Y, Luo LH, Li S and Yang C: miR-17 inhibitor suppressed osteosarcoma tumor growth and metastasis via increasing PTEN expression. Biochem Biophys Res Commun 444: 230-234, 2014.
9. Yue LU, Xiang JY, Sun P, Yao YS, Sun ZN, Liu XP, Wang HB, Shen Z and Yao RY: Relationship between HSP70 and ERBB2 expression in breast cancer cell lines regarding drug resistance. Anticancer Res 36: 1243-1249, 2016.
10. Yu X, Li Z, Chan MT and Wu WK: microRNA deregulation in keloids: An opportunity for clinical intervention? Cell Prolif 48: 626-630, 2015.
11. Pan JY, Zhang F, Sun CC, Li SJ, Li G, Gong FY, Bo T, He J, Hua RX, Hu WD, et al: miR-134: A human cancer suppressor? Mol Ther Nucleic Acids 6: 140-149, 2017.
12. Cao Q, Liu F, Ji K, Liu N, He Y, Zhang W and Wang L: MicroRNA-381 inhibits the metastasis of gastric cancer by targeting TMEM16A expression. J Exp Clin Cancer Res 36: 29, 2017.
13. Yu X, Li Z, Yu J, Chan MTV and Wu WKK: MicroRNAs predict and modulate responses to chemotherapy in colorectal cancer. Cell Prolif 48: 503-510, 2015.
14. Pei K, Zhu JJ, Wang CE, Xie QL and Guo JY: MicroRNA-185-5p modulates chemosensitivity of human non-small cell lung cancer to cisplatin via targeting ABCC1. Eur Rev Med Pharmacol Sci 20: 4697-4704, 2016.
15. Yu S, Qin X, Chen T, Zhou L, Xu X and Feng J: MicroRNA-106b-5p regulates cisplatin chemosensitivity by targeting polycystic kidney disease-2 in non-small-cell lung cancer. Anticancer Drugs 28: 852-860, 2017.
16. Gang H, Pan J, Ye Z, Fang B and Wei C: Overexpression of miR-216b sensitizes NSCLC cells to cisplatin-induced apoptosis by targeting c-Jun. Oncotarget 8: 104206-104215, 2017.

17. Azarbarzin S, Feizi MAH, Safaralizadeh R, Kazemzadeh M and Fateh A: The value of miR-383, an intronic miRNA, as a diagnostic and prognostic biomarker in intestinal-type gastric cancer. Biochem Genet 55: 244-252, 2017.

18. Bucay N, Sekhon K, Yang T, Majid S, Shahryari V, Hsieh C, Mitsui Y, Deng G, Tabatabai ZL, Yamamura S, *et al*: MicroRNA-383 located in frequently deleted chromosomal locus 8p22 regulates CD44 in prostate cancer. Oncogene 36: 2667-2679, 2017.

19. Shang Y, Zang A, Li J, Jia Y, Li X, Zhang L, Huo R, Yang J, Feng J, Ge K, *et al*: MicroRNA-383 is a tumor suppressor and potential prognostic biomarker in human non-small cell lung caner. Biomed Pharmacother 83: 1175-1181, 2016.

20. Ma H, Liu B, Wang S and Liu J: MicroRNA-383 is a tumor suppressor in human lung cancer by targeting endothelial PAS domain-containing protein 1. Cell Biochem Funct 34: 613-619, 2016.

21. Tan W, Liao Y, Qiu Y, Liu H, Tan D, Wu T, Tang M, Zhang S and Wang H: miRNA 146a promotes chemotherapy resistance in lung cancer cells by targeting DNA damage inducible transcript 3 (CHOP). Cancer Lett 428: 55-68, 2018.

22. Wagenaar SS: New WHO-classification of lung and pleural tumors. Ned Tijdschr Geneeskd 143: 984-990, 1999 (In Dutch).

23. Tsim S, O'Dowd CA, Milroy R and Davidson S: Staging of non-small cell lung cancer (NSCLC): A review. Respir Med 104: 1767-1774, 2010.

24. Livak KJ and Schmittgen TD: Analysis of relative gene expression data using real-time quantitative PCR and the 2(-Delta Delta C(T)) method. Methods 25: 402-408, 2001.

25. Lee S, Kopp F, Chang TC, Sataluri A, Chen B, Sivakumar S, Yu H, Xie Y and Mendell JT: Noncoding RNA NORAD regulates genomic stability by sequestering PUMILIO proteins. Cell 164: 69-80, 2016.

26. National Research Council (US) Committee for the Update of the Guide for the Care and Use of Laboratory Animals: Guide for the Care and Use of Laboratory Animals. 8th edition. National Academies Press, Washington DC, 2011.

27. Shanker M, Willcutts D, Roth JA and Ramesh R: Drug resistance in lung cancer. Lung Cancer (Auckl) 1: 23-36, 2010.

28. Panwar B, Omenn GS and Guan Y: miRmine: A database of human miRNA expression profiles. Bioinformatics 33: 1554-1560, 2017.

29. Ludwig N, Leidinger P, Becker K, Backes C, Fehlmann T, Pallasch C, Rheinheimer S, Meder B, Stähler C, Meese E and Keller A: Distribution of miRNA expression across human tissues. Nucleic Acids Res 44: 3865-3877, 2016.

30. Wan P, Chi X, Du Q, Luo J, Cui X, Dong K, Bing Y, Heres C and Geller DA: miR-383 promotes cholangiocarcinoma cell proliferation, migration, and invasion through targeting IRF1. J Cell Biochem 119: 9720-9729, 2018.

31. Dong P, Xiong Y, Yu J, Chen L, Tao T, Yi S, Hanley SJB, Yue J, Watari H and Sakuragi N: Correction: Control of PD-L1 expression by miR-140/142/340/383 and oncogenic activation of the OCT4-miR-18a pathway in cervical cancer. Oncogene 38: 3972, 2019.

32. Zhao S, Gao X, Zang S, Li Y, Feng X and Yuan X: MicroRNA-383-5p acts as a prognostic marker and inhibitor of cell proliferation in lung adenocarcinoma by cancerous inhibitor of protein phosphatase 2A. Oncol Lett 14: 3573-3579, 2017.

33. Mu X, Wu H, Liu J, Hu X, Wu H, Chen L, Liu W, Luo S and Zhao Y: Long noncoding RNA TMPO-AS1 promotes lung adenocarcinoma progression and is negatively regulated by miR-383-5p. Biomed Pharmacother 125: 109989, 2020.

34. Piovani G, Savio G, Traversa M, Pilotta A, De Petro G, Barlati S and Magri C: De novo 1Mb interstitial deletion of 8p22 in a patient with slight mental retardation and speech delay. Mol Cytogenet 7: 25, 2014.

35. Chi C, Murphy LC and Hu P: Recurrent copy number alterations in young women with breast cancer. Oncotarget 9: 11541-11558, 2018.

36. Tsubaki M, Ogawa N, Takeda T, Sakamoto K, Shimaoka H, Fujita A, Itoh T, Imano M, Satou T and Nishida S: Dimethyl fumarate induces apoptosis of hematopoietic tumor cells via inhibition of NF-κB nuclear translocation and down-regulation of Bcl-xL and XIAP. Biomed Pharmacother 68: 999-1005, 2014.

37. Viatour P, Merville MP, Bours V and Chariot A: Phosphorylation of NF-kappaB and IkappaB proteins: Implications in cancer and inflammation. Trends Biochem Sci 30: 43-52, 2005.

38. Chen Y, Wang D, Peng H, Chen X, Han X, Yu J, Wang W, Liang L, Liu Z, Zheng Y, *et al*: Epigenetically upregulated oncoprotein PLCE1 drives esophageal carcinoma angiogenesis and proliferation via activating the PI-PLCε-NF-κB signaling pathway and VEGF-C/Bcl-2 expression. Mol Cancer 18: 1, 2019.

39. Bravo-Cuellar A, Hernández-Flores G, Lerma-Díaz JM, Domínguez-Rodríguez JR, Jave-Suárez LF, De Célis-Carrillo R, Aguilar-Lemarroy A, Gómez-Lomeli P and Ortiz-Lazareno PC: Pentoxifylline and the proteasome inhibitor MG132 induce apoptosis in human leukemia U937 cells through a decrease in the expression of Bcl-2 and Bcl-XL and phosphorylation of p65. J Biomed Sci 20: 13, 2013.

40. Yao Y, Yang B, Cao H, Zhao K and Chen X: RBM24 stabilizes hepatitis B virus pregenomic RNA but inhibits core protein translation by targeting the terminal redundancy sequence. Emerg Microbes Infect 7: 86, 2018.

41. Hua WF, Zhong Q, Xia TL, Chen Q, Zhang MY, Zhou AJ, Tu ZW, Qu C, Li MZ, Xia YF, *et al*: RBM24 suppresses cancer progression by upregulating miR-25 to target MALAT1 in nasopharyngeal carcinoma. Cell Death Dis 7: e2352, 2016.

42. Xu E, Zhang J, Zhang M, Jiang Y, Cho SJ and Chen X: RNA-binding protein RBM24 regulates p63 expression via mRNA stability. Mol Cancer Res 12: 359-369, 2014.

43. Zhang Q, Wang YZ, Zhang W, Chen X, Wang J, Chen J and Luo W: Involvement of cold inducible RNA-binding protein in severe hypoxia-induced growth arrest of neural stem cells in vitro. Mol Neurobiol 54: 2143-2153, 2016.